Research Journal of Recent Sciences ISSN 2277-2502
Vol. **4(2),** 120-129, February **(2015)** *Res.J.Recent Sci.*

Application of artificial Intelligence in Generating Artificial Accelerograms using Kanai-Tajimi model

Gharehbaghi S.A.[1*] and Mohaghegh A.[2]
[1*] Civil Engineering Dept., K. N. Toosi university of technology, Tehran, IRAN
[2]K.N. Toosi University of Technology, Tehran, IRAN

Available online at: www.isca.in, www.isca.me
Received 30th March 2014, revised 15th June 2014, accepted 7th September 2014

Abstract

Several civil engineering activities need dynamic time history analysis or other numerical simulations. In such cases, it is very important to have accurate and adequate accelerograms. However in most situations, there is not enough data for a specific site or region. Many powerful methods are developed in order to generate artificial earthquake records. This paper is aimed at combining non-stationary Kanai-Tajimi model and artificial neural networks for generation artificial earthquake records. More precisely, two radial basis neural networks (RBF) are applied to conjecture filter parameters from response spectrum. Moreover, in non-stationary Kanai-Tajimi method one needs to guess proper pattern for filter parameters, based on human intelligence or experience. These patterns vary from one accelerogram to other because of record characteristics. General regression neural network (GRNN) are used in order to find better approximation of filter parameters without use of human judgment, applied to original non-stationary Kanai-Tajimi method. A new method in selecting proper Moving-Time-Window size, used in non-stationary Kanai-Tajimi method is presented in this paper. Finally, RBFs are trained and used in artificial accelerogram generation for a given velocity response spectrum. Three earthquake records, including Bam 2003, Gheshm 2005 and Zanjiran 1994, occurred in Iran are used to verify proposed method. At the end, the performance of proposed method is investigated statistically. Statistical results indicate the accuracy of the proposed method.

Keywords: Artificial accelerogram, non-stationary Kanai-tajimi model, radial basis neural network, general regression neural network, gaussian white noise, moving-time-window.

Introduction

A safe and economic design of heavy industrial structures like dams, cooling towers, nuclear power plants and high-rise buildings requires special considerations. It is suitable to use spectrum analysis method in some of above mentioned structures. On the other hand, structural engineers have to simulate dynamical systems, using time history analysis under specific circumstances. Spectrum analysis method is used to compute responses, required for designing. However, spectrum analysis is unable to provide time information about structural responses and behavior during time. Dynamic time history analysis requires accurate and adequate accelerograms. Each accelerogram must consider geological conditions of the region and have the closest spectrum to actual spectrum. Due to the lack of real seismic accelerograms and increasing use of dynamic time history analysis, generating artificial earthquake records plays an important role.

Because of random nature of earthquakes, many researchers have studied stochastic models and it was extensively used in earthquake simulation[1-2]. The stationary filtered white noise model of earthquake by Kanai and Tajimi has attracted considerable attention[3-4]. Ahmadi and Fan proposed a method, based on non-stationary variables and frequency content[5]. Rofooei et al applied this model with some changes and generated artificial accelerograms[6]. Nonetheless, Ghodrati, Bagheri and Fadavi and Ghodrati and Bagheri developed innovative methods based on non-stationary Kanai-Tajimi model and wavelet analysis[7-8].

Artificial neural networks have a wide range of usage in various research disciplines. Depending on type a neural network, it can be used for pattern recognition, classification or function approximation. Ghaboussi and Lin and Lin and Ghaboussi have valuable researches regarding artificial neural networks[9-10]. Their main idea is: if the response spectrum computation is considered as a direct problem, determining an accelerogram regarding the response spectrum will be the reverse problem which can be solved using artificial neural network. Many another researches are done by Li and Han, Bargi, Rahami and Loux and Ghodrati and Bagheri, Ghodrati, Bagheri and Seyed Razaghi[11-14].

The purpose of this paper is to present an innovative method in order to create several artificial accelerograms, having appropriate consistency with the target spectrum. In this study, a combined method, based on non-stationary Kanai-Tajimi model and artificial neural networks is presented. This method tries to minimize the effect of human intelligence and engineering judgments, used in non-stationary Kanai-Tajimi model, increasing performance and reducing errors in generating artificial earthquake records. Because of learning capabilities of a radial basis function neural network (RBF), this type of neural network is used to estimate the knowledge of the inverse mapping from response spectrum to earthquake accelerogram. More precisely, two artificial neural networks are applied to conjecture the filter parameters from response spectrum. Rofooei et al[6] used Moving-Time-Window technique in non-stationary Kanai-Tajimi model. This technique is applied in the present paper. Moreover, a new method suggested for selecting window size automatically. As well as, General regression neural network (GRNN) are used instead of regression analysis in non-stationary Kanai-Tajimi model. In the next section, the original non-stationary Kanai-Tajimi model is presented.

The non-stationary Kanai-Tajimi model

The generalized Kanai-Tajimi model is based on Kanai's investigation on the frequency content of various earthquake records[3]. Tajimi proposed equation (1) for the spectral density function of strong ground motion with a distinct dominant frequency[4].

$$G(\omega) = \frac{\left[1+4\xi_g^2(\omega/\omega_g)^2\right]}{\left[1-(\omega/\omega_g)^2\right]^2+4\xi_g^2(\omega/\omega_g)^2} G_0 \qquad (1)$$

In which ξ_g and ω_g are the ground damping ratio and frequency respectively and G_0 is the constant power spectral intensity of the bed rock excitation. In practice these parameters should be estimated from local earthquake records or geological features. Kanai-Tajimi power spectral density function, corresponding with damping ratio is presented in figure-1.

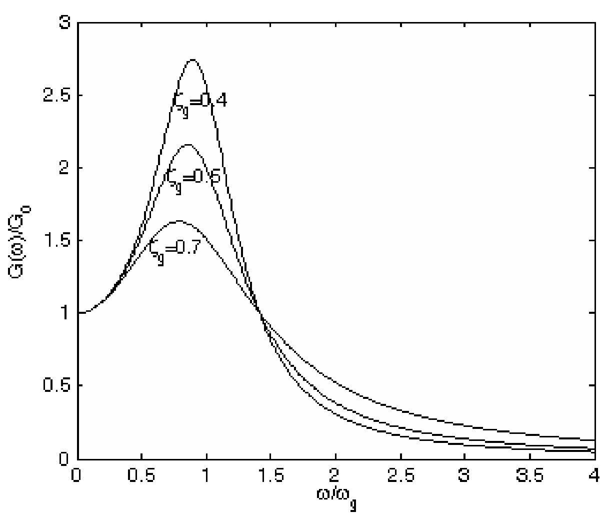

Figure-1
Kanai-Tajimi power spectral density function

The Kanai–Tajimi power spectral density function may be interpreted as an ‘ideal white noise’ excitation at the bedrock level filtered through the overlaying soil deposits at a site.

This model assumes that earthquakes are stationary phenomena, which is not correct. A stationary process in mathematics is a process that does not change its character with respect to time[15], while, earthquake records have intense non-stationary characteristic. Ahmadi and Fan[5] suggested a model, governed by equations (2) and (3), capturing the non-stationary nature of earthquake in order to overcome the drawbacks of Kanai-Tajimi model.

$$\ddot{X}_f + 2\xi_g(t)\omega_g(t)\dot{X}_f + \omega_g^2(t)X_f = n(t) \qquad (2)$$

$$\ddot{X}_g = -\left(2\xi_g(t)\omega_g(t)\dot{X}_f + \omega_g^2(t)X_f\right)e(t) \qquad (3)$$

Where X_f is filtered response, $\omega_g(t)$ is time dependent ground frequency, $\xi_g(t)$ is effective ground damping coefficient, $\ddot{X}_g$ is output ground acceleration, e(t) is the amplitude envelope function and n(t) is a stationary Gaussian white noise process.[5] Rofooei et al (2001) generated a new method according to this model to generate artificial earthquake records. In this method, $\omega_g(t)$ and e(t) are estimated, using Moving-Time-Window procedure. This method is summarized as following [6]:

i. Time duration of strong ground motion is determined. ii. Optimum size of Moving-Time-Window is computed. iii. So as to estimate e(t), Moving-Time-Window is used as a time interval and moved from the beginning to the end of the accelerogram. The standard deviation of each Moving-Time-Window is calculated, using equation (4) and assigned to the center point of current Moving-Time-Window.

$$\sigma = \sqrt{E[X^2] - E[X]^2} \qquad (4)$$

Where, X is the value of accelerogram points residing in Moving-Time-Window. A smooth algebraic time function $\sigma_a(t)$ is fitted to the time variation of the standard deviation. This function varies from one accelerogram to another and needs to be selected using human intelligence or experience. The amplitude envelope function, defined in equation-5 is calculated.

$$e(t) = C_0.\sigma_a(t) \qquad (5)$$

Where, C_0 is a constant that will be determined by normalizing the mean intensity of the synthetic accelerograms to the intensity of actual accelerogram. In order to compute $\omega_g(t)$, Moving-Time-Window procedure is used again. As the first step, the zero-crossing rate of accelerogram is calculated for each Moving-Time-Window, using equation-6 and assigned to the center point.

$$\hat{F}_c(t) = \frac{\left(\text{Number of zero crossing within the time interval } \left(t\pm\frac{t_w}{2}\right)\right)}{t_w} \qquad (6)$$

Where t_w is the size of window. Again, a suitable algebraic time-dependent function is fitted to the variation of the zero-crossing rate $\hat{F}_{ca}(t)$. Selecting the pattern of this function is important and needs human intelligence. The ground frequency function is calculated as:

$$\omega_g(t) = \pi \hat{F}_{ca}(t) \tag{7}$$

Now, it is possible to generate artificial accelerograms. At first, a Gaussian white noise is generated and after that, equations-2 and 3 are solved for $\ddot{X}_g$.

It is very important to select suitable time-window size. It should be sufficiently short to capture the rapid changes in frequency content and sufficiently long to provide stable estimation of parameters and to capture significant low frequency components. Attention was also given to the stability of the parameter estimations for each record. In mentioned study, the optimal time-window size is selected based on the frequency content of the earthquake using a trial and error method[6].

The artificial Neural Networks

In recent years, a wide range of researches for solving problems based on pragmatic data in which there is either no solution or a hard-to-deal-with one. One of the solutions is using the artificial neural networks which transfer the rule or the knowledge beyond the data to the network structure, processing the practical data. Hence these systems are called intelligent systems, because they learn the general rule through calculating numeric data and instances. These systems try for modeling the human's brain neuro-synaptic structure. There are diverse kinds of networks. They all are formed by neurons and connections between them. In fact each node is a calculative unit of the network which obtains inputs, processes them and finally provides the outputs. The performed process by neuron can include the simplest one such as collecting inputs to the most complex calculations. On the other hand, connections define the quality of data transfer among neurons. In General form, connections can be either unilateral or bilateral. The researches have shown that only one neuron with many inputs is not enough for solving the problems. In this case, one needs several neurons to function in a parallel way. One or more neurons juxtaposed to each other form a layer of the network. A network can contain one or more layers. The meaning of training in neural networks is computing all weights of all connections between neurons[16].

In 1985, Powel achieved a method based on radial function for multi-variant internal-exploration. In 1988, Broomhead and Lowe employed this approach in neural networks and according to that the neural networks based on radial based function which are herein mentioned as RBF were created. RBF is a three-layer feed-forward neural network which able to process each non-linear mapping with the aid of changing parameters by using the non-linear transform functions in the neurons. RBF architecture accelerates the training speed by lining making in determining the weight of connections. The RBF networks have recently been used for practical issues like pattern recognition, signal processing, etc. RBF networks have several advantages rather than multi-layer perceptron networks. They usually train much faster than perceptron networks and they create a better decision-making circumstance[17].

Radial basis function neural network (RBF): A typical RBF neural network, having three-layer architecture is shown in figure-2.

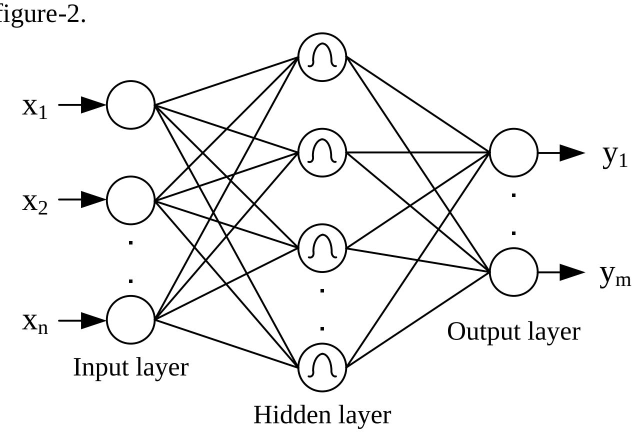

Figure-2
RBF Structure

The first layer is the input one. There is no processing in the input layer. The second layer or the hidden layer creates a non-linear conformity between the input space and a larger area in which the patterns turn to the linear separable ones. Finally the third layer produces the weight sum along with the linear outputs. For function approximation, above mentioned RBF network seems to be effective. However, in pattern recognition problems, sigmoid function should be used as transform function for output layer neurons in order to produce 0 or 1 values[17].

A unique feature of RBF is process that is done in hidden layer. Thus the radial basis function is used as transform function for hidden layer neurons. The most usual radial function form is defined as:

$$\phi(r) = e^{-\frac{r^2}{2\sigma^2}} \tag{8}$$

Equation-8 indicates a normal Bell-shaped curve as shown in figure-3. Where, r is the numeric amount of the distance length from the cluster center. The variant σ is defined as width or the radial of the Bell-shaped and in compulsorily cases it is sometimes assessed empirically.

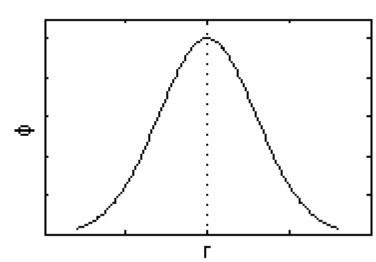

Figure-3
Bell-Shaped curve, used as transform function in hidden layer of RBF neural network

The estimated distance to the cluster center is usually of Euclidean type. When a neuron receives an input pattern, the mentioned distance can be calculated through equation-9.

$$r_j = \sqrt{\sum_{i=1}^{n} \left(x_i - w_{ij}\right)^2} \quad (9)$$

Where x_i is input and w_{ij} is weight between neuron i and j. Thus the j[th] neuron output in the hidden layer is as follow:

$$\phi_j = e^{-\frac{\sum_{i=1}^{n}\left(x_i - w_{ij}\right)^2}{2\sigma^2}} \quad (10)$$

Training neural networks with radial function is a kind of supervised training, which needs a set of so called "training data", including a complete set of inputs and corresponding outputs. Hidden layer of a RBF network has some weighted units which are corresponding to the vector pointing out the cluster center. The weights of hidden layer can be calculated through traditional methods like "K-Mean" algorithm. After training the hidden layer through the training algorithms, the last stage of training the output layer will be fulfilled through using a standard technique of gradient descent[17].

General Regression Neural Network (GRNN): This type of artificial neural network has been developed for identifying and modeling practical problems by Specht[18]. The structure of this network is very similar to RBF. The main characteristic of GRNN is the ability to estimate any function by having a set of input and output data, used as training set[17]. Suppose a function with n inputs of the form $\vec{x} = (x_1, x_2, \ldots, x_n)$ and one output of the form y. The expected average of an output can be calculated by having a single input of $\vec{x}$ through equation-12.

$$\bar{y}(\vec{x}) = \frac{\int_{-\infty}^{\infty} y \times PDF(\vec{x}, y)\,dy}{PDF(\vec{x})} \quad (12)$$

This equation includes the function $PDF(\vec{x}, y)$ which is the joint probability density function $\vec{x}$ and y and it computes the probability when output is equal to y and input is equal to $\vec{x}$. The probability density functions are estimated through the sum of Gaussian functions. Therefore the conditional probability functions can be estimated by placing a Gaussian function center on each existed inputs in a training set and multiplying these Gaussian functions by each output corresponding to inputs. Finally, it can be calculated through equation-13.

$$\hat{y} = \frac{\sum_{p=1}^{P} y_p e^{-\frac{d_p^2}{2\sigma^2}}}{\sum_{p=1}^{P} e^{-\frac{d_p^2}{2\sigma^2}}} \quad (13)$$

In this equation it is supposed that p couples of data are available in the training set. Each couple includes a training pair, containing an input vector $\overrightarrow{x_p} = (x_{1p}, x_{2p}, \ldots, x_{np})$ and the output y_p corresponding to the input vector $\overrightarrow{x_p}$. d_p indicates the Euclidean distance between the new input vector and p^{th} input vector in training set. In order to compute output of a new input vector, the distance of this vector and all other existed input vectors in the training set will be calculated, afterward the amount of each Gaussian distribution based on its distance to new input will be estimated and multiplying by each output corresponding to input vectors. The denominator of equation (13) indicates the summation of outputs of the Gaussian functions[17].

The proposed Model: As mentioned before, this research present a creative technique with admixture non-stationary Kanai-Tajimi model and artificial neural networks for generating artificial earthquake records which has good performance and minimum effect of human intelligence or judgment. In order to reduce human intelligence, two artificial neural networks, called ANN-I and ANN-II have been trained to receive the velocity response spectrum as the input and render the smooth time functions of zero-crossing rate and standard deviation as the output. In other word, $\hat{F}_{ca}(t)$ and $\sigma_a(t)$ will be obtained using artificial neural networks. This means that there is no need of judgment or experience for selecting a good pattern for all smoothed functions. In fact, they are obtained automatically. In the next step, one Gaussian white noise is made for obtaining each artificial accelerogram. Then, equations-2 and 3 will be solved for $\ddot{X}_g$. A schematic algorithm of proposed method is presented in figure-4.

Suggested method has two general stages: Architecture designing and training the neural networks, Modeling and producing the artificial accelerograms.

In this research, two radial basis function neural network (RBF) have been used. In order to train neural network, we need pairs of data, input and its corresponding output. The inputs of the networks are the velocity response spectrum which can be calculated through the typical methods. The outputs of ANN-I and ANN-II are smooth time functions of zero-crossing rate and the standard deviation, respectively. Outputs are computed using the "Moving Time Window" technique. Thus, a window size is selected for each training accelerogram and the time-dependent parameters such as zero-crossing rate and standard deviation are calculated, using equation-4 and 6, within each window and allocated to the central point. Finally, a smooth algebraic time function is fitted to the time variations.

As noted before, the important point in using the Moving-Time-Window technique is to choose the appropriate size of the window; this size should be small enough to be able not only to capture the rapid changes of the frequency content but also to compute stable approximation of parameters in time interval. Meanwhile it should be large enough to be able to capture the lower frequency content. Because of using different accelerograms for training the neural networks, the size of each Moving-Time-Window should be calculated properly and automatically. In this research a novel method is used for selecting the size of Moving-Time-Window. In this method, the Fast Fourier transform of each accelerogram is investigated. To achieve a logical balance between the upper and lower frequencies, a proportion of the energy from the whole accelerogram is chosen. This proportion can be changed to achieve the best responses. Then the frequency f_n in which the accelerogram reaches to this specific level of its whole energy will be determined from Fast Fourier spectrum. The corresponding period will be used as the size of the window. In figure-5 different samples of window size selection is presented. The outcomes of this research indicate that using the standard of forty percent of the whole energy is a good selection in order to achieve better results.

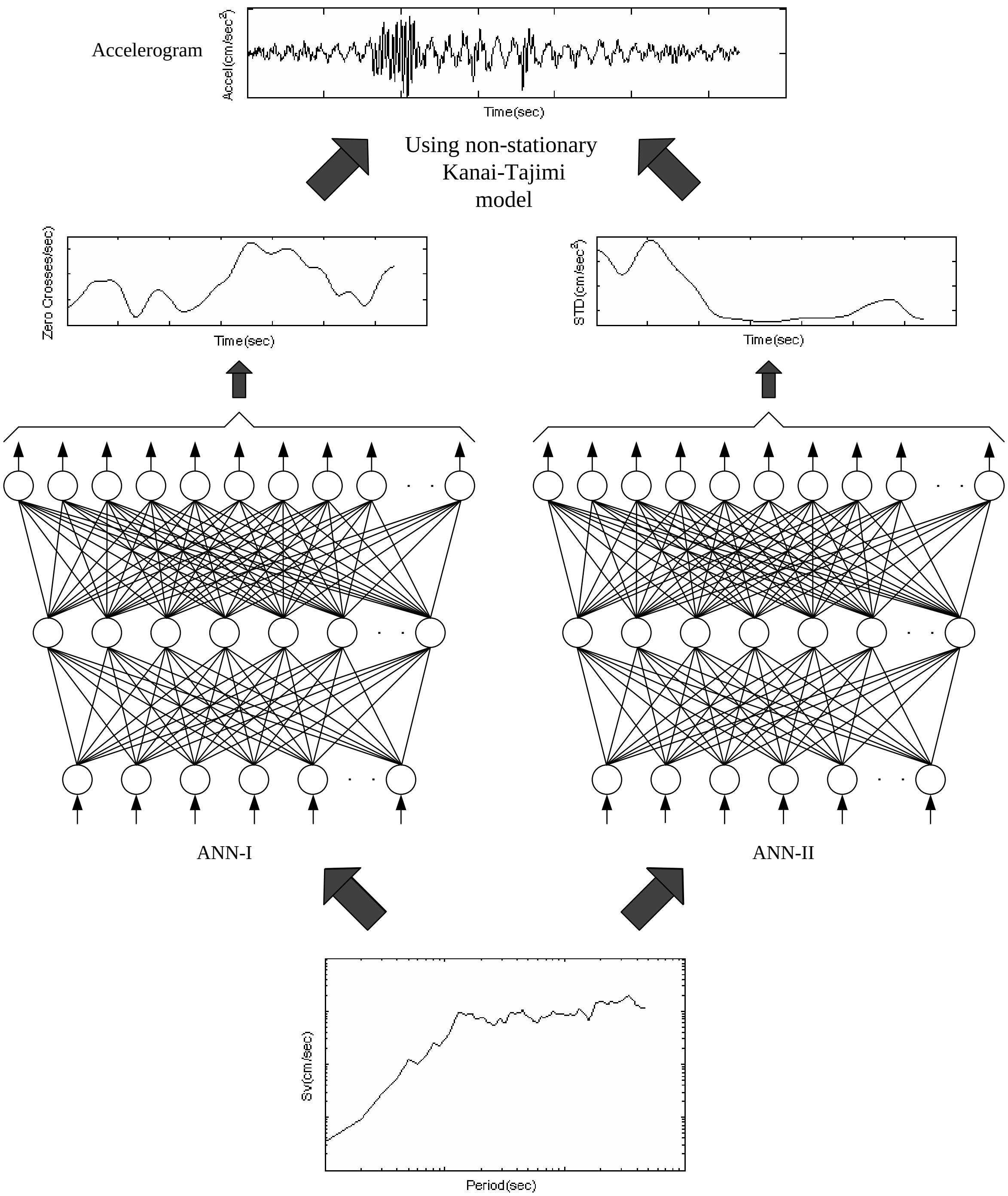

Figure-4
The suggested method for generating artificial accelerogram

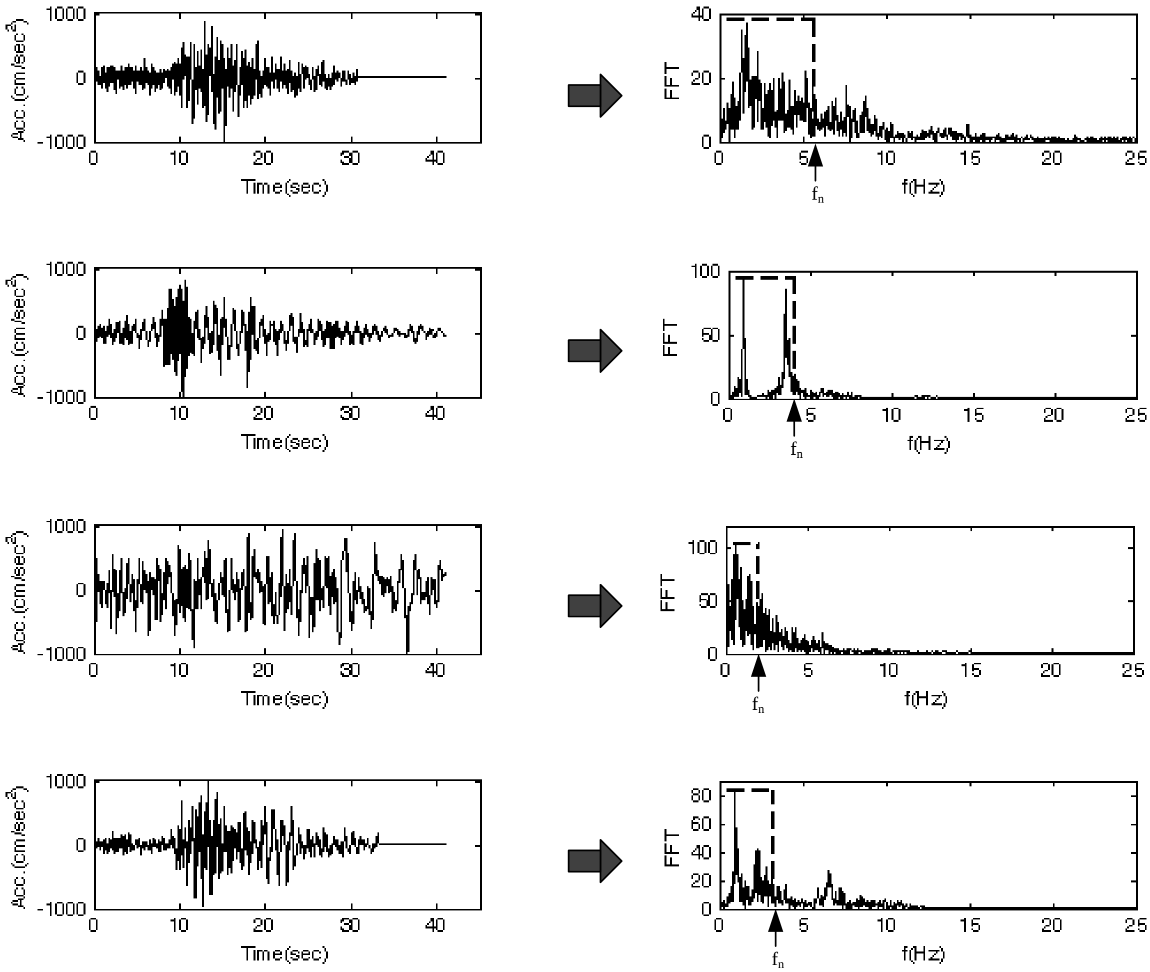

Figure-5
Different samples of window size selection; Left: accelerogram, Right: Fast Fourier Transform

After selecting window size and computing the time-dependent parameters of filter, a smooth algebraic time function is fitted to these time variations. As mentioned before, these functions vary between diverse accelerograms. For training ANN-I and ANN-II, because of using different accelerograms two GRNN are applied instead of regression analysis. In the recent years it has been shown that the multilayer perceptron networks with a hidden layer, containing sigmoid transform functions in the middle layer and linear transform functions in the output layer are able to estimate any give function with a specific error tolerance[16]. In the other hand, amongst radial basis function neural networks, GRNN networks are used in order to approximate functions. GRNN is able to estimate any function by having a set of input and output data. In present study, two GRNN, called GRNN-I and GRNN-II are applied. The input of GRNNs is the time. The outputs of GRNN-I and GRNN-II are smooth time functions of zero-crossing rate and the standard deviation, respectively. In order to train GRNN-I a set of time and time variation of zero-crossing rate, as input and output data are given to this network. Similarly, GRNN-II receives a set of time and time variation of standard deviation for training. Now, GRNN-I and GRNN-II are able to provide a proper and smooth approximation for zero-crossing rate and standard deviation. In figure-6 different samples of smooth function approximation by GRNNs is presented.

Velocity response spectrum and two smooth time functions, zero-crossing rate and standard deviation, are prepared for each accelerogram in training set. In the next step two RBF networks are trained for these data. Afterwards, ANN-I and ANN-II are able to provide a proper and smooth approximation for standard deviation and zero-crossing rate as outputs, in return for receiving velocity response spectrum as input.

After network training, to produce artificial earthquake records, a spectrum corresponded to each test accelerogram is calculated and is presented to ANNs as input. ANN-I is presented zero-crossing rate smooth time function and ANN-II standard deviation smooth function in output. Then amplitude envelope function $e(t)$ and ground frequency function $\omega_g(t)$ are calculated using relations (5) and (7), respectively.

For computing the envelope function C_0 is considered 1. Then, a time series Gaussian white noise $n(t)$, must be created. Next, the differential equation-2 is solved. For solving this equation the numerical Runge-Kutta method is used which is able to compute and illustrate error, simultaneously. By solving that and determining the filtered responses and also placement in equation-3, the artificial ground accelerations are generated.

Numerical simulations

In order to investigate the performance of the improved and mechanized method, three earthquake records are used separately and numerous artificial accelerograms are generated from each actual record. The preliminary characteristics of records are presented in table-1.

All used accelerograms have been recorded in 0.005s time intervals, which is very time consuming in order to be analyzed and simulated. Therefore a method has been used for decreasing the number of pairs in each accelerogram. Considering Shannon sampling theorem which has represented if a signal has finite energy, the minimum sampling rate is equal to two samples per period of the highest frequency component of the signal.[15] So, when the sampling period of a signal is 0.02, the sampled signal will have the capacity of the correct display up to the frequency of $25\ hertz$. Regarding the natural frequency specifications of the earthquakes, this assumption is sufficient in order to represent earthquake signal in 0.02s intervals.

In other hand, a new earthquake record is obtained from actual one, using $2^{11} = 2048$ points. There are two possible conditions; in the first case, the number of all remaining points is less than 2048. In this circumstance, enough number of zero acceleration points are added to the record. In the second case, the number of all remaining points is greater than 2048. In such situations, the number of data in record is reduced, using Trifunac and Brady algorithms[20]. This algorithm considers only ninety five percent of whole energy of earthquake as strong duration. Finally, These records were scaled with their peak ground acceleration to $1g$.

In training step, networks input are velocity response spectrum in the period interval of $0.01\ sec$ to $4.6\ sec$ in 460 points, which is computed by applying Newmark method with average acceleration $\left(\beta = \frac{1}{4}, \gamma = \frac{1}{2}\right)$[21].

Ground damping coefficient $\xi_g(t)$, depends on geotechnical conditions of each region. However, $\xi_g(t)$ is considered to be equal to 0.35, 0.35 and 0.30 for Bam, Gheshm and Zanjiran, respectively.

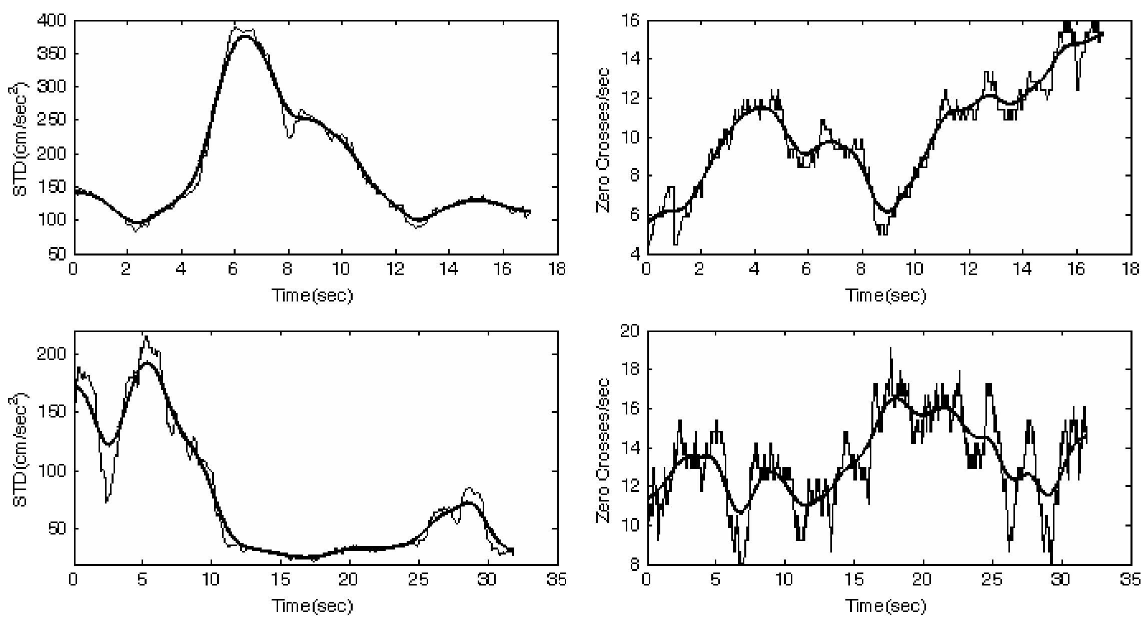

Figure-6
Different samples of smooth function approximation by GRNNs; Left: standard deviation with time and smooth curve, Right: zero-crossing rate with time and smooth curve

Table-1
Characteristic of actual earthquake records[19]

Earthquake	Date	Station	Magnitude (Ms)	Data	Comp
Bam	26.12.2003	Nosrat Abad	6.7	Train	V
Gheshm	27.11.2005	Bandar-e-khamir	5.9	Test	V
Zanjiran	20.06.1994	Farashband	5.9	Test	V

The performance of proposed method is investigated statistically. For this purpose, fifty artificial accelerograms are generated and comparison has been made between actual response spectrum and the average of synthetic accelerograms spectral values. To calculate the spectrum, Newmark method is used and damping coefficient of the single degree of freedom structure is assumed to be equal to five percent. Actual record of each earthquake is presented in figures-7 through 9. In each case, one artificial accelerogram is presented and statistical results of fifty artificial records are computed and compared with actual one. Numerical simulations show that the proposed method has an acceptable accuracy, regarding actual results.

More statistical analysis is done, using fifty artificial accelerogram for each actual record. The mean value and standard deviation of velocity response spectrum are computed through equations-14 and 15:

$$\bar{V}(T_0, \xi_0) = E[S_v(T_0, \xi_0)] \tag{14}$$

$$\sigma_V(T_0, \xi_0) = \sqrt{E\{(S_v(T_0, \xi_0) - \bar{V})^2\}} \tag{15}$$

The absolute maximum velocity response spectrum and the minimum velocity response spectrum, defined as (16) and (17), have been evaluated among all the artificial accelerograms.

$$V_{max}\,(T_0, \xi_0) = max\{S_v(T_0, \xi_0)\} \tag{16}$$

$$V_{min}\,(T_0, \xi_0) = min\{S_v(T_0, \xi_0)\} \tag{17}$$

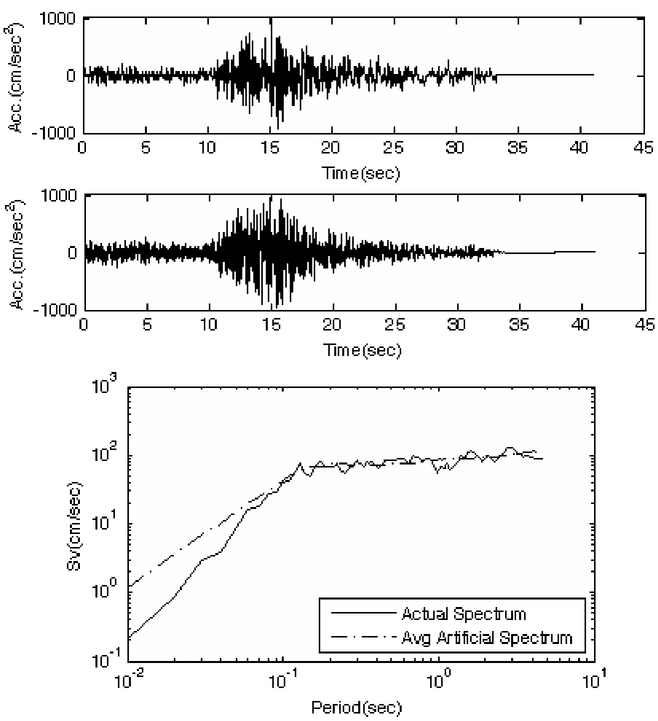

Figure-7
(a) Actual accelerogram of Bam (2003) V, (b): A typical artificial accelerogram, (c): Actual velocity response spectrum versus average artificial spectrum

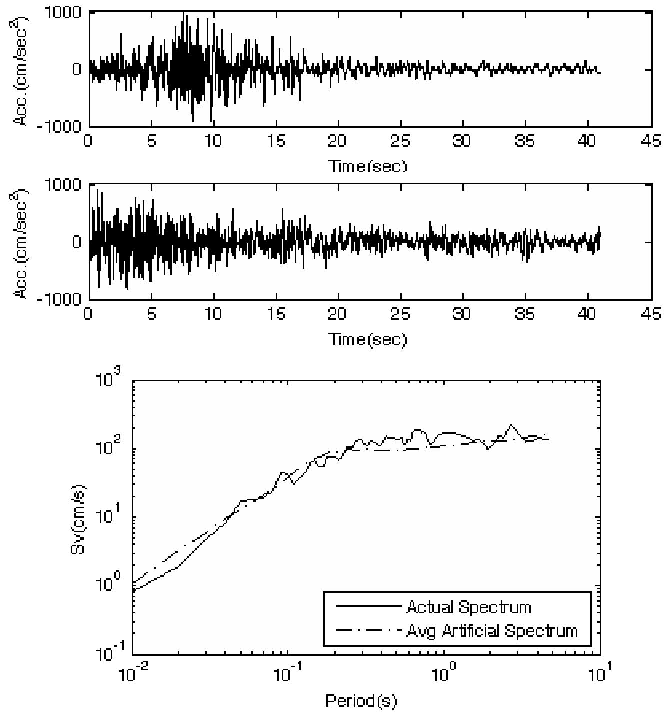

Figure-8
(a) Actual accelerogram of Gheshm (2005) V, (b): A typical artificial accelerogram, (c): Actual velocity response spectrum versus average artificial spectrum

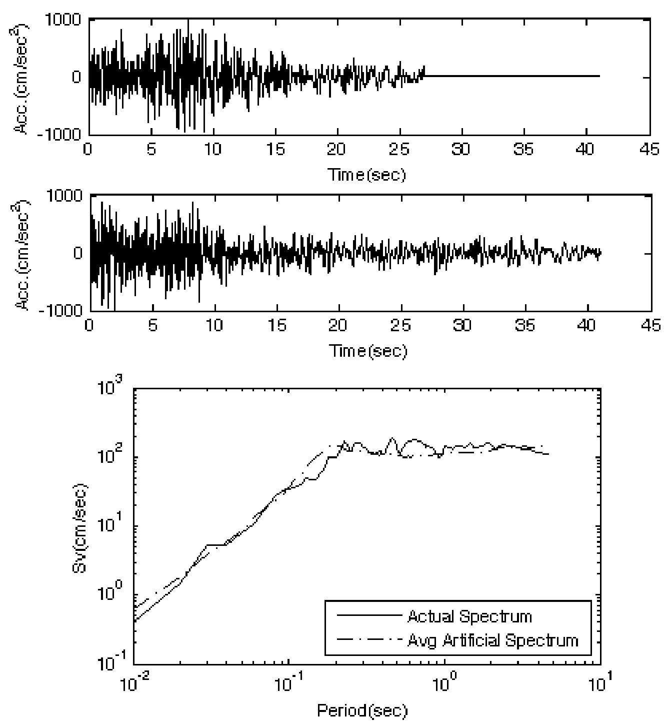

Figure-9
(a) Actual accelerogram of Zanjiran (1994) V, (b): A typical artificial accelerogram, (c): Actual velocity response spectrum versus average artificial spectrum

Spectral values, including actual earthquake record spectrum, mean spectrums from fifty artificial accelerograms, absolute maximum velocity response spectrum, absolute minimum velocity response spectrum and statistical band, surrounding of mean values are plotted in figures-9 through 11.

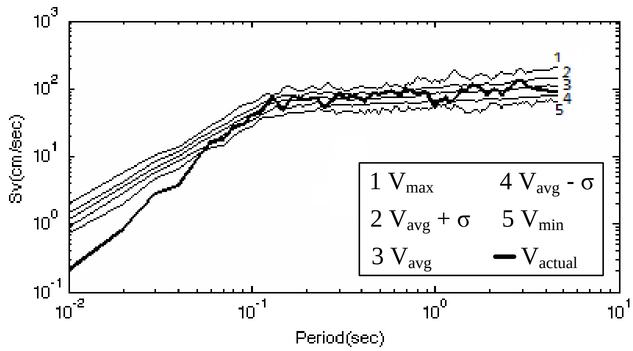

Figure-9
Comparison between actual response spectrum and statistical results for Bam earthquake (2003)

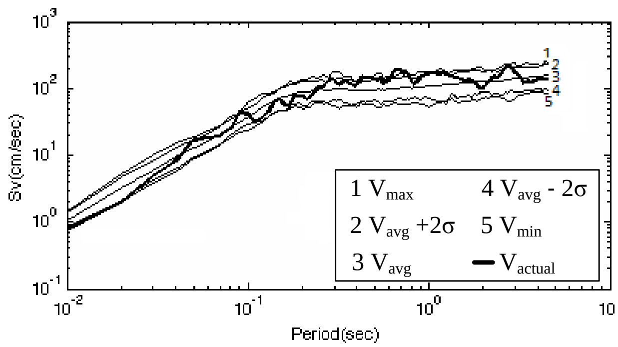

Figure-10
Comparison between actual response spectrum and statistical results for Gheshm earthquake (2005)

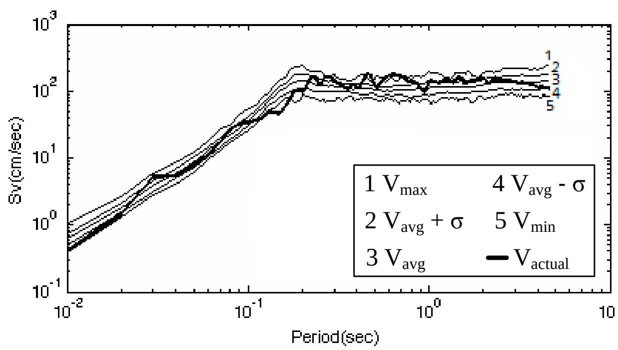

Figure-11
Comparison between actual response spectrum and statistical results for Zanjiran earthquake (1994)

Conclusion

In this paper a combined method, based on non-stationary Kanai-Tajimi model and artificial neural networks is presented. The proposed method uses artificial neural networks in order to conjecture the filter parameters from response spectrum. Moreover, present study tries to reduce human intelligence and experience needed in selecting proper patterns for smooth function approximation of standard deviation and zero-crossing rate diagrams. More study is performed to adopt the Moving-Time-Window technique, used in the original method with proposed method in order to reduce human judgment in selecting the size of Moving-Time-Window. Therefore, the proposed method is automatic and is able to be used as standalone software. Statistical results show the accuracy of the proposed method. Maximum amount of error occurs for stiff structures with a period less than 0.05s, which is not common in ordinary buildings, so this automated method can be applied for ordinary buildings safely.

The findings in this study are in accordance with Khodaie Mahmoodi et al[23], Sheeba and Rangarajan[24], Ali Shah etal[25], Samadi et al[26] and Nadeem Saher[27].

References

1. Jennings P.C, Housner G.W and Tsai N.C, Simulated Earthquake motions, *Earthquake engineering research Laboratory*, **(1968)**

2. Housner G.W. and Jennings P.C, Generation of artificial earthquakes, *Journal of the Engineering Mechanics Division, Proceedings of ASCE*, 90 (EM1), 113–150 **(1964)**

3. Kanai K., Semi-empirical formula for the seismic characteristics of the ground, *Earthquake Research Inst., Univ. Tokyo Bull.*, **35,** 309-325 **(1957)**

4. Tajimi H., A statistical method of determining the maximum response of a building structure during an earthquake, In : Proc. 2nd WCEE, Vol.II, Tokyo: Science Council of Japan, 781-798 **(1960)**

5. Ahmadi G. and Fan F.G., Nonstationary Kanai-Tajimi model for El Centro 1940 and Mexico City 1985 earthquake, *Probabilistic Engineering Mechanics*, **5,** 171-181 **(1990)**

6. Rofooei F.R., Mobarake A.A. and Ahmadi G., Generation of Artificial Earthquake Records with a Nonstationary Kanai-Tajimi Model, Engineering Structures, **23,** 827-837 **(2001)**

7. Ghodrati Amiri G., Bagheri A. and Fadavi Amiri M., New method for generation of artificial ground motion by a nonstationary Kanai-Tajimi model and wavelet transform, *Structural Engineering and Mechanics*, **26(6),** 709-723 **(2007)**

8. Ghodrati Amiri G. and Bagheri A., Simulation of earthquake records using combination of wavelet analysis and nonstationary Kanai-Tajimi model, *Structural Engineering and Mechanics*, **33(2)**, 179-191 **(2009)**

9. Ghaboussi J. and Lin C.J., New method of generating

spectrum compatible accelerograms using neural networks, *Earthquake Engineering Structural Dynamics*, **27,** 377-396 **(1998)**

10. Lin C.J. and Ghaboussi J., Generating multiple spectrum compatible accelerograms using stochastic neural networks, *Earthquake Engineering Structural Dynamics*, **30,** 1021-1042 **(2001)**

11. Lee S.C. and Han S.W, Neural-network-based models for generating artificial earthquakes and response spectra, *Computers and Structures*, **80,** 1627–1638 **(2002)**

12. Bargi K.H, Rahami H. and Loux C, Generation of artificial accelerograms using neural networks for data of IRAN, *Journal of faculty of engineering (University of Tehran)*, **36(2),** 177-183 **(2002)**

13. Ghodrati Amiri G. and Bagheri A., Application of wavelet multiresolution analysis and artificial intelligence for generation of artificial earthquake accelerograms, *Structural Engineering and Mechanics*, **28(2),** 153-166 **(2008)**

14. Ghodrati Amiri G., Bagheri A. and Seyed Razaghi, S.A., Generation of Multiple Earthquake Accelerograms Compatible with Spectrum via the Wavelet Packet Transform and Stochastic Neural Networks, *Journal of Earthquake Engineering*, **13(7),** 899-915 **(2009)**

15. Robert J. Marks ll, Introduction to Shannon sampling and interpolation theory, Springer-Verlag New York, **(1991)**

16. Menhaj M., Calculation Intelligence: Neural Network, Amirkabir University, Iran, **(1998)**

17. Picton P., Neural network, second edition, Grassroots Series, **(2000)**

18. D.F.A. Specht, A general regression neural network, *IEEE Transactions on Neural Networks*, **2,** 568-576 **(1991)**

19. Building and Housing Research Center (BHRC), Available from URL: http://www.bhrc.ac.ir/., **(2014)**

20. Naeim F., The Seismic Design Handbook, Van Nostrand, **(1999)**

21. Chopra A.K., Dynamics of Structures, Englewood Cliffs, NJ: Prentice-Hall **(1995)**

22. Clough R.W. and Penzien J., Dynamics of Structures, Second Edition, McGraw-Hill, **(1993)**

23. Reza Khodaie Mahmoodi, Sedigheh Sarabi Nejad and Mehdi Ershadi sis , Expert Systems and Artificial Intelligence Capabilities Empower Strategic Decisions : A Case study, *Res. J. Recent Sci.*, **3(1),** 116-121 **(2014)**

24. Blesslin Sheeba T. and Rangarajan P., SOC Implementation of Hybrid Cryptography Techniques using Hight and RC4 Algorithm, *Res. J. Recent Sci.*, **3(5),** 65-70 **(2014)**

25. Jawad Ali Shah, I.M. Qureshi, Amir A. Khaliq and Hammad Omer, Sparse Signal Recovery based on Hybrid Genetic Algorithm, *Res. J. Recent Sci.*, **3(5),** 86-93 **(2014)**

26. Hamid Reza Samadi, Asghar Teymoorian and Mostafa GhasemiLandslide analysis to estimate probability occurrence of earthquakes by software ArcGIS in central of Iran, *Res. J. Recent Sci.*, **3(5),** 104-109 **(2014)**

27. Faisal Nadeem Saher, Nasly M.A., Tuty Asmawaty Binti Abdul Kadir, Nasehir Khan E.M. Yahaya, Wan Mohd Faizal Wan Ishak Harnessing Floodwater of Hill Torrents for Improved Spate Irrigation System Using Geo-Informatics Approach, *Res. J. Recent Sci.*, **3(1),** 14-22 **(2014)**